

MOLECULAR SIMULATIONS OF GOLD NANOPARTICLES COATED WITH SELF-ASSEMBLED ALKANETHIOLATE MONOLAYERS

Brian J. Henz*
U.S. Army Research Laboratory
Aberdeen Proving Ground, MD 21005

James W. Fischer
HPTi
Aberdeen Proving Ground, MD 21005

Michael R. Zachariah
Departments of Mechanical Engineering and Chemistry
University of Maryland
College Park, MD 20742

Abstract

In order to utilize the novel electrical, magnetic, optical, and physical properties of coated metal nanoparticles, one must be able to efficiently predict the nanoparticle size-dependent properties and to fabricate consistently sized nanoparticles. Both of these goals can be obtained through the use of numerical simulation. In this work the gold nanoparticle and nanoparticle/self-assembled monolayer systems have been analyzed with a physically accurate and computationally efficient numerical simulation. The simulation model and method are described in the following paper.

1. Introduction

In this work we have used molecular dynamics (MD) simulations to study gold nanoparticles with alkanethiolate SAMs. This material system is an extensively researched system in the study of SAMs because of its wide applicability and the wealth of experimental data available. The MD algorithm is used because it can efficiently simulate large numbers of atoms with the desired accuracy. This is an important consideration when large numbers of atoms are to be analyzed. We have combined accurate MD potentials for each of the subsystems, namely the gold nanoparticle and the alkanethiolate polymer chain. The system is then analyzed by varying parameters such as temperature, SAM chain length, and the density of adsorbed chains.

*Presenting author

2. Computational Procedure

Molecular dynamics (MD) studies of alkanethiolate SAMs on gold surfaces are well documented [9, 24, 29]. These studies have been limited to flat gold surfaces or fixed gold atoms in a nanocrystallite [12, 15]. In addition to, and in support of these previous MD simulations, quantum mechanical simulations have been used to study gold clusters with short alkanethiolate SAMs. Interestingly, the quantum mechanical findings have suggested that the gold crystal lattice is appreciably affected by the adsorbed ligand [7] with an increase in the Au-Au bond length of up to 20%. The quantum mechanical results suggest that the MD simulations should include dynamic gold atoms in order to accurately model the nanoparticle/SAM system. Without the simulation of dynamic gold atoms, the changes that occur to the surface is not considered.

2.1. Software and Optimization

The software for this project was chosen based on its current capabilities, extensibility, and parallel performance. The software used needs to be extensible because of the many unique computational algorithms required in this project. Some of the unique algorithms include computing the radial pressure distribution inside of the nanoparticle and use of uncommon potentials. For MD simulations it was determined that the Large-scale Atomic/Molecular Massively Parallel Simulator (LAMMPS) from Sandia National Laboratories was the best choice as it is open source, widely used, and has massively parallel capabilities [19]. LAMMPS is open source software allowing for the easy integration of new routines to the application, thus providing the required extensibility.

Report Documentation Page

Form Approved
OMB No. 0704-0188

Public reporting burden for the collection of information is estimated to average 1 hour per response, including the time for reviewing instructions, searching existing data sources, gathering and maintaining the data needed, and completing and reviewing the collection of information. Send comments regarding this burden estimate or any other aspect of this collection of information, including suggestions for reducing this burden, to Washington Headquarters Services, Directorate for Information Operations and Reports, 1215 Jefferson Davis Highway, Suite 1204, Arlington VA 22202-4302. Respondents should be aware that notwithstanding any other provision of law, no person shall be subject to a penalty for failing to comply with a collection of information if it does not display a currently valid OMB control number.

1. REPORT DATE 01 NOV 2006		2. REPORT TYPE N/A		3. DATES COVERED -	
4. TITLE AND SUBTITLE Molecular Simulations Of Gold Nanoparticles Coated With Self-Assembled Alkanethiolate Monolayers				5a. CONTRACT NUMBER	
				5b. GRANT NUMBER	
				5c. PROGRAM ELEMENT NUMBER	
6. AUTHOR(S)				5d. PROJECT NUMBER	
				5e. TASK NUMBER	
				5f. WORK UNIT NUMBER	
7. PERFORMING ORGANIZATION NAME(S) AND ADDRESS(ES) U.S. Army Research Laboratory Aberdeen Proving Ground, MD 21005				8. PERFORMING ORGANIZATION REPORT NUMBER	
9. SPONSORING/MONITORING AGENCY NAME(S) AND ADDRESS(ES)				10. SPONSOR/MONITOR'S ACRONYM(S)	
				11. SPONSOR/MONITOR'S REPORT NUMBER(S)	
12. DISTRIBUTION/AVAILABILITY STATEMENT Approved for public release, distribution unlimited					
13. SUPPLEMENTARY NOTES See also ADM002075., The original document contains color images.					
14. ABSTRACT					
15. SUBJECT TERMS					
16. SECURITY CLASSIFICATION OF:			17. LIMITATION OF ABSTRACT UU	18. NUMBER OF PAGES 8	19a. NAME OF RESPONSIBLE PERSON
a. REPORT unclassified	b. ABSTRACT unclassified	c. THIS PAGE unclassified			

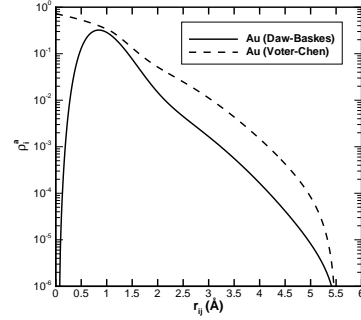
Although LAMMPS is massively parallel, and easy to use, there appeared to be some inefficiencies in the software, that if corrected, could provide improved performance. A PET (User Productivity Enhancement and Technology Transfer) project at the U.S. Army Research Laboratory was underway at the time of this effort to look at this issue. The project team discovered many opportunities for performance enhancements through extensive profiling and benchmarking. Each of the following enhancements provided some improvement but together they provided a 3.5x improvement in run time for the alkanethiolate SAM coated gold nanoparticle model. Some of the biggest improvements came from reducing array accesses, using temporary variables, restructuring of if-else blocks, and eliminating conditional blocks by using C++ templates. Some other improvements came from machine specific changes to the code that assisted the compiler such as the manual unrolling of inner loops by four.

2.2. Simulating the Gold Substrate

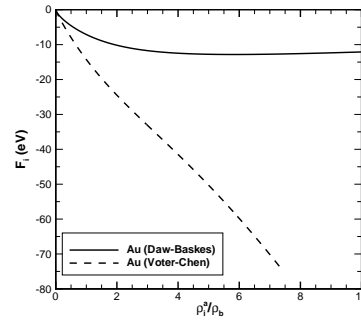
When explicitly considering the gold substrate as dynamic atoms, the embedded atom method (EAM) [4, 5, 18] and the effective medium (EM) [11, 20, 25] potentials have received the most attention, are computationally efficient, and provide accurate results in MD simulations under many conditions. These methods use empirical embedding functions that originate from density functional theory (DFT) and have been successfully used to model many of the physical properties of gold. Since the embedding functions are empirical, they are computationally efficient and yet still accurate enough for many purposes. This efficiency makes it possible for large numbers of atoms to be modeled, and thus analysis of realistically sized systems is feasible. We have decided to use the EAM for modeling the gold substrate because of its accuracy and the extensions available for modeling surfaces, such as the extended EAM (XEAM) [13]. In the EAM, the potential function is a combination of the embedding energy and pair potential terms as in equation 1. The actual data that is used in this work is given in Figure 1 along with a second dataset from Voter and Chen [28]. A detailed discussion of the method as used in this work can be found in Daw et al. [4, 5].

$$E_{tot} = \sum_i F_i(\rho_{h,i}) + \frac{1}{2} \sum_i \sum_{j(\neq i)} \phi_{ij}(R_{ij}) \quad (1)$$

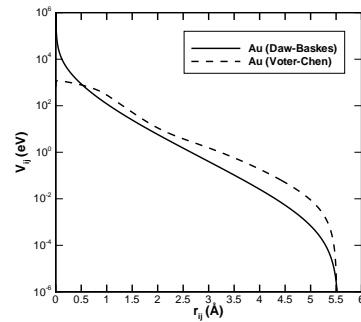
The gold nanoparticle model begins as a simple sphere with a face centered cubic (FCC) lattice structure as seen in figure 2(a). The model is then heated to 1000 K, or above the melting temperature, and held for a short time of ~ 10 ns. After the nanoparticle has been melted for about 10 ns



(a) Electron density



(b) Embedding energy where ρ_i has been scaled by $\rho_b = 0.025$ for auu3 and 0.15 for Voter-Chen.



(c) Pair potential

Figure 1. Gold (Au) EAM potentials from LAMMPS [19]. Distances are measured in Angstroms (Å) and energy is given in electron volts (eV)

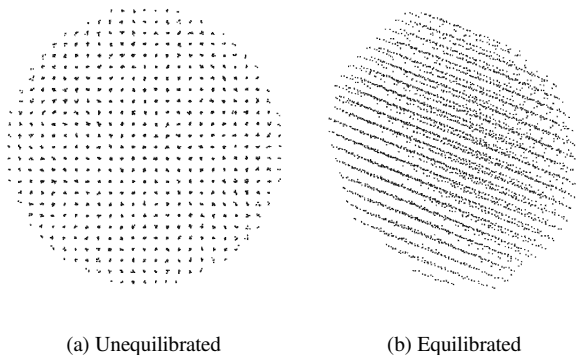


Figure 2. Equilibrated and Unequilibrated

the model is slowly cooled to the desired simulation temperature. This process minimizes the energy of the system and provides the most accurate representation of the equilibrated nanoparticle possible. The equilibrated gold nanoparticle in figure 2(b) has large facets and is no longer spherical. This geometry is expected as it minimizes the energy of the system as opposed to the perfect sphere.

2.3. Modeling the Alkanethiolate Chain

SAMs are formed by the spontaneous adsorption of self-assembling molecules on a solid substrate. A SAM's thermal stability and structural properties are governed by the substrate-head molecular and intrachain interactions in the chemisorbed layer. The chemical identity of the SAM tail molecule governs the surface properties of the coated metal and affects interactions with the environment. Examples of SAM systems include alkanethiols or dialkyl disulfides on gold and silver, organosilicon on hydroxylated silicon wafers, and carboxylic acids on aluminum.

The alkanethiolate polymer chain that coats the gold nanoparticle in this work may be modeled with a range of complexity. For MD simulations the three methods available are the high-accuracy/high computational requirement all-atom model, the less accurate/lower computational requirement united atom method, and the coarse grained bond model. For instance, consider the CH_2 molecule that makes up the backbone of the alkanethiolate chain. When using the all-atom model the numerical simulation must consider three particles for each molecule. Using the united atom model only one particle is simulated for each molecule [10], and with the coarse grained model multiple molecules are grouped together into one particle with perhaps five or more CH_2 molecules grouped into one simulated particle [6, 17, 27]. The model chosen for a particular simulation depends greatly upon the level of detail required in the simulation and corresponding results of interest. For the

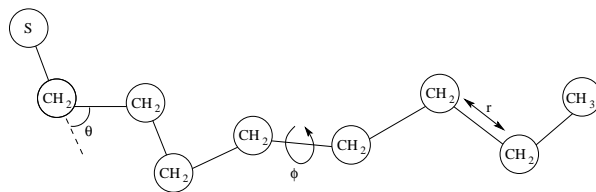


Figure 3. Sample alkanethiolate chain with 8 carbon atoms along the backbone.

simulations in this work we have chosen the united atom method, which is computationally more efficient than the all atom method yet provides enough accuracy for any anticipated quantitative analysis.

The modeling of the alkanethiolate chain using the united atom model is consistent with many of the Au-SAM system published results. An example of the alkanethiolate polymer chain model used in this work is shown in Figure 3. The potentials used in the united atom model include a bending potential for the S-C-C bond and the C-C-C bond. The bending potential can be modeled as either a flexible bond with a form similar to equation 2 or as a stiff bond where the angle is held constant. There is a dihedral potential for X-C-C-X bonds, where X can be either S or C and takes the form of equation 3. There are two common methods used in the literature to model the bond lengths along the chain. The bond lengths along the chain can be held constant [24] with the RATTLE [2] algorithm or they can be modeled as harmonic bonds [17, 21] as given in equation 4. Using a harmonic bond to describe the C-C and S-C backbone bonds allows the distance between the backbone atoms to change while not allowing the bonds to break.

$$U_{bending}(\theta) = \frac{1}{2}k_{\theta}(\theta - \theta_0)^2 \quad (2)$$

$$U_{dihedral}(\phi) = \sum_{i=0}^5 a_i \cos^i(\phi) \quad (3)$$

$$U_{bond}(r) = \frac{1}{2}k_r(r - r_0)^2 \quad (4)$$

The values of the parameters used in this work are as follows. For the C-C bond stretch model $k_r = 30.349 \frac{eV}{\text{\AA}^2}$, $r_0 = 1.53 \text{\AA}$, and for S-C bond stretching $k_r = 35.594 \frac{eV}{\text{\AA}^2}$, $r_0 = 1.82 \text{\AA}$ [21]. The bond bending potential for the C-C-C angle is $k_{\theta} = 8840.0419 \frac{eV}{deg^2}$, $\theta_0 = 109.5 deg$, and for the S-C-C angle $k_{\theta} = 8840.0419 \frac{eV}{deg^2}$, $\theta_0 = 114.4 deg$ [24]. The parameters for the dihedral bonds from equation 3 are $a_0 = 0.0961661$, $a_1 = 0.125981$, $a_2 = -0.1359773$, $a_3 = -0.0317102$, $a_4 = 0.271954$, $a_5 = -0.326414$ [24].

2.4. Binding of Sulfur to Gold

The binding of the head sulfur atom of an alkanethiolate chain to the gold substrate is of great interest as it affects the location, orientation, movement, and desorption of chains from the substrate [3,7,16]. Much effort has been devoted to finding accurate potentials for simulating the sulfur binding energy. Determining the potential parameters in MD simulations requires the use of expensive ab initio calculations such as DFT [3,7]. The most published potentials resulting from these calculations are the 12-3 potential [8], used most commonly in Monte Carlo (MC) simulations of alkanethiolates on gold [9,24] and the Morse potential, used in many of the MD simulation studies [9,14,16,29]. In addition to the issue of which potential best describes the binding between SAM head-group and substrate, the possibility of SAM mobility is also an important consideration [3]. On curved surfaces, as opposed to flat surfaces, the boundary conditions that restrict lateral movement on the surface are not present and so chain mobility is a primary consideration.

3. Computational Results

In this section we will present our findings from the MD simulations studied. Of interest, is the observation that for gold nanoparticles, adsorbed SAMs modify the crystallinity of the gold atoms near the nanoparticle surface. First, the structural change needs to be quantified, and then the ability to predict the structural change from parameters such as temperature, alkanethiolate chain length, surface coverage, etc. can be investigated. The following discussions will focus on the observed properties of the simulated nanoparticle.

In order to study the affects of the SAM on the nanoparticle we have computed the pair correlation function, diffusion coefficients, and radial pressure and density distributions. Each of these results will give some insight into what changes the nanoparticle surface experiences by the addition of the adsorbed SAMs. For instance, the diffusion coefficient will be used to compute the mobility of the SAMs that are adsorbed on the surface, and also the mobility of the gold atoms near the surface of the nanoparticle. This information will indicate the phase of the materials at and on the surface and also help in predicting if nucleation of the SAMs may occur, where under low surface coverage conditions the chains will form dense groups and uneven surface coverage. The density distribution is used to find the depth to which the sulfur atoms penetrate the surface of the gold nanoparticle. The density distribution is used to define a corrugation factor that describes the change in the size of the nanoparticle core.

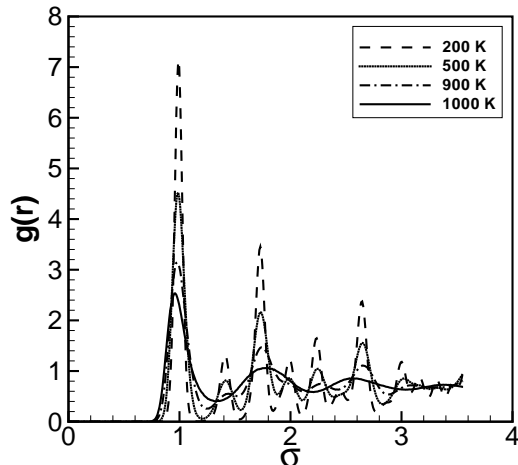


Figure 4. Pair correlation function for bare 5nm gold nanoparticle. Note the change in shape and number of peaks between 900 K and 1000 K. This change indicates that a phase change from solid to liquid has taken place.

3.1. Pair Correlation Function

The pair correlation function $g(r)$ is the number of atoms a distance r from a given atom compared with the number at the same distance in an ideal gas at the same density [1]. The pair correlation therefore is used to provide insight into the structure of the nanoparticle, from highly crystalline with sharp peaks for nearest neighbors, next-nearest neighbors, and so on, to liquids with peaks at multiples of the nearest neighbor distance. Equation 5 is used to compute the pair correlation function $g(r)$.

$$g(r) = \frac{V}{N^2} \left\langle \sum_i \sum_{j \neq i} \delta(\vec{r} - \vec{r}_{ij}) \right\rangle \quad (5)$$

In equation 5 V is the volume of the simulation bounds, N is the number of simulated particles, and δ is the delta function.

The pair correlation function is useful because the ensemble average of any pair function may be expressed as a function of the pair correlation function. Some results for the bare 5nm gold nanoparticle are given in figure 4. These results indicate a phase transition occurs in the nanoparticle from a crystalline solid at 900 K to a liquid at 1000 K. It can therefore be assumed that a 5nm gold nanoparticle melts in this temperature range.

3.2. Diffusion

The diffusion coefficients computed here are used to quantify the mobility of the SAMs on the gold nanoparticle surface. The diffusion coefficient of the alkanethiolate chain is computed by considering the mean squared distance traveled by the sulfur head group during a simulation. The diffusion coefficient, D , is computed using equation 6.

$$\frac{\partial \langle r^2(t) \rangle}{\partial t} = 2dD \quad (6)$$

In equation 6, d is the number of dimensions available for atomic diffusion, in this case 3, t is elapsed time, and $\langle r^2(t) \rangle$ is the mean squared displacement (MSD) of the atoms being tracked.

In addition to studying the diffusion of the sulfur atoms we have also considered the diffusion of the gold surface atoms that are bound to the sulfur atoms. This information is used to determine whether or not the sulfur atoms are moving over the surface atoms or with the surface atoms. If the sulfur is moving over the nanoparticle surface, they are considered mobile and may nucleate on the surface. If the gold surface is diffusing at a similar rate then the gold on the surface may be carrying the sulfur with it, and the chains are not moving in relation to the gold surface. Figure 5 contains the MSD results for alkanethiolate SAMs adsorbed on a gold nanoparticle at 300 K and full surface coverage. These results give a MSD value for the sulfur head group of $8.05 \cdot 10^{-7} \text{ cm}^2/\text{s}$ and for the gold surface atoms of $9.75 \cdot 10^{-8} \text{ cm}^2/\text{s}$. The difference in diffusion coefficients is about one order of magnitude, indicating that the alkanethiolate chains are relatively mobile over the nanoparticle surface.

Another study performed using the calculation of diffusion coefficients is the temperature dependence of the diffusivity vs. temperature. By comparing the logarithm of the diffusion coefficient of the SAMs for various temperatures it should be possible to see regions of linear increases in $\ln(D)$ vs. $1/T$. A linear curve would indicate an Arrhenius distribution. In figure 6 there are three distinct linear regions with slopes of -260.9 , -461.6 , and -4565.3 , indicating three phases in the alkanethiolate SAM.

3.3. Radial Density Distribution

Thus far the computed results have shown the the 5nm bare nanoparticle has a melting temperature between 900 K and 1000 K (pair correlation function), the SAMs are mobile over the gold surface (diffusion coefficient), and that there are three possible phases between 100 K and 800 K. The next calculation, namely the radial density, is required as part of the radial pressure calculation. The radial density distribution is used to determine where the edge of the gold

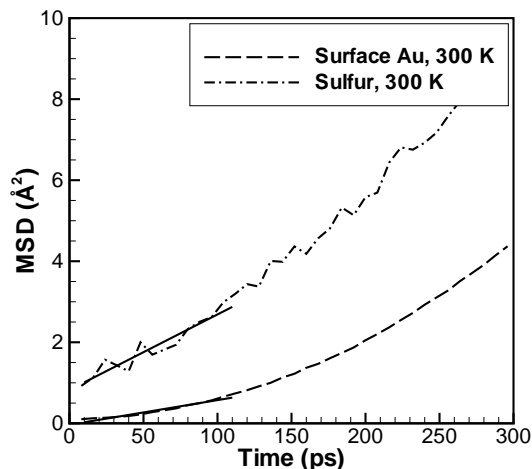


Figure 5. The MSD of sulfur head group atoms and the gold surface atoms in a SAM coated nanoparticle. These results indicate that the SAMs are moving freely over the gold surface.

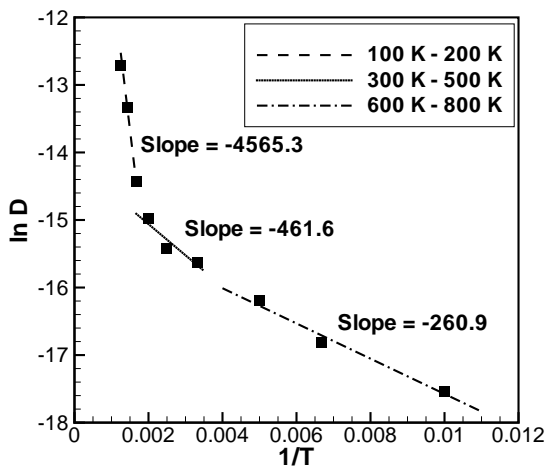


Figure 6. The activation energy for SAM mobility is estimated by the slope of $\ln(D)$ vs. $1/T$ for various temperatures between 100 K and 800 K.

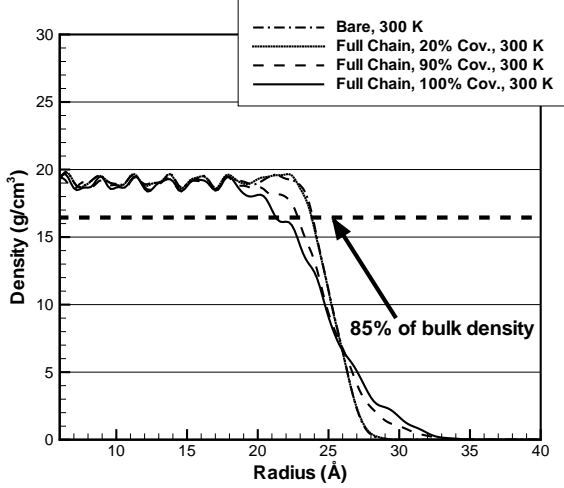


Figure 7. Radial density of gold in alkanethiolate SAM coated gold nanoparticle for various surface coverage amounts.

nanoparticle core occurs. For bare nanoparticles the change in density will be abrupt at the surface, but for coated particles the slope will be lower if the SAMs penetrate into the gold surface. The SAM penetrating into the surface was not initially assumed because past work simulating alkanethiolate coated gold nanoparticles has assumed that the gold atoms do not move because of the interactions with the SAMs [15]. With the parallel computing capabilities of LAMMPS it was possible to model the SAMs and the gold atoms as dynamic particles. This allowed for an investigation of whether or not the gold atoms are affected by the SAMs. When computing the radial density as shown in figure 7 it became apparent that the atoms near the surface of the gold nanoparticle are in fact moving and corrugating the surface.

In an attempt to quantify the surface corrugation we have defined a corrugation factor, C , that is defined as

$$C = \frac{r(\rho = 0.85\rho_{bulk})_{bare} - r(\rho = 0.85\rho_{bulk})_{coated}}{r(\rho = 0.85\rho_{bulk})_{bare}} \quad (7)$$

where $r(\rho = 0.85\rho_{bulk})$ is the radius where the computed gold density is 85% of the density of bulk gold. This definition of the corrugation factor will be 0.0 for the bare gold nanoparticle and up to 1.0 for a gold nanoparticle with impurities or a dissolved solute. For coated gold nanoparticles with various percentages of surface coverage the corrugation factor has been computed and is listed in table 1.

Table 1. Computed corrugation factors for alkanethiolate SAM coated gold nanoparticles.

Coverage	C
Bare	0.000
10%	0.004
20%	0.004
70%	0.012
80%	0.018
90%	0.043
100%	0.107

3.4. Radial Pressure Distribution

It is known that small droplets have an elevated internal pressure due to compressive forces arising from the surface tension. In these MD simulations the radial pressure distribution inside of the nanoparticle is computed using the Irving-Kirkwood pressure tensor [26]. The Irving-Kirkwood pressure tensor, equation 8, has contributions from two terms, namely the kinetic (P_K) and configurational (P_U).

$$P_N(r) = P_K(r) + P_U(r) \quad (8)$$

P_N indicates the normal component of the pressure tensor. The kinetic term is dependent upon the radial density distribution, $\rho(r)$, and the system temperature, equation 9.

$$P_K(r) = k_B T \rho(r) \quad (9)$$

where k_B is Boltzmann's constant. The configurational term is dependent upon atomic interactions that act across the radius of interest, as seen in figure 8. In equation 10 the calculation of the configurational term is defined.

$$P_U(r) = - (4\pi r^3) \sum_k |\vec{r} \cdot \vec{r}_{ij}| \frac{1}{r_{ij}} \frac{du(r_{ij})}{dr_{ij}} \quad (10)$$

In equation 10 \vec{r}_{ij} is the vector between the interacting atoms that crosses radius r of the sphere of interest. $u(r_{ij})$ is the potential energy of the atomic interaction and so $\frac{du(r_{ij})}{dr_{ij}}$ is the force of the interaction. Using this calculation, the radial pressure distribution for bare 5nm gold nanoparticles at temperatures between 200 K and 1000 K have been computed and plotted in figure 9.

The pressure results in figure 9 show that the pressure at the surface of a nanoparticle slightly above the melting temperature is about 5900 bar. This result is used with the Young-Laplace equation, equation 11, to compute the nanoparticle surface tension.

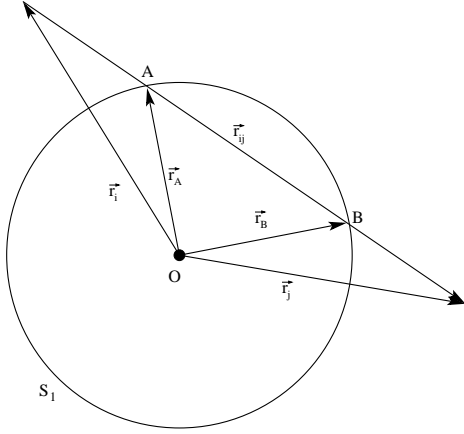


Figure 8. Illustration of forces and position vectors used to calculate configurational term in Irving-Kirkwood pressure tensor.

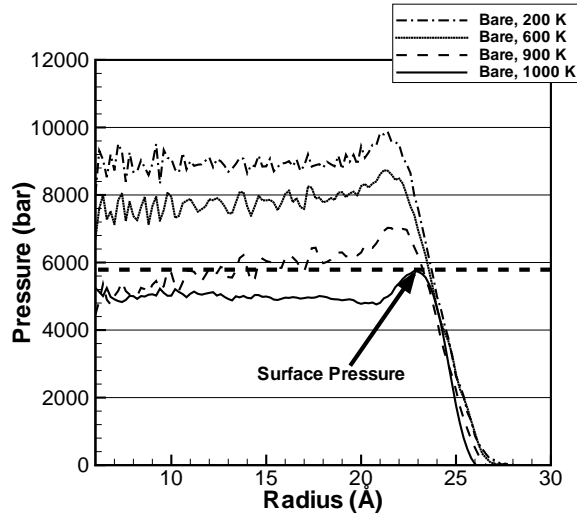


Figure 9. Radial distribution of the normal component of the Irving-Kirkwood pressure tensor for bare 5nm gold nanoparticles at various temperatures.

$$\Delta P = \frac{2\gamma}{r} \quad (11)$$

where γ is the surface tension, r is the nanoparticle radius, and ΔP is the difference in pressure between the nanoparticle and the surrounding medium, in this case a vacuum. Assuming a pressure of 5900 bar and a radius of 2.5nm the computed surface tension is about $738 \frac{mN}{m}$. This result compares favorably to the published data for bulk gold at the melting temperature of $742 \frac{mN}{m}$. Another calculation from Widom et al [22] is used to calculate the surface tension from the MD simulation with equation eq:widom.

$$\gamma_i^3 = -\frac{1}{8} (p_{r_2} - p_{r_1})^2 \int_{r_1}^{r_2} r^3 \frac{dp_N(r)}{dr} dr \quad (12)$$

In equation 12, p_{r_2} and p_{r_1} are the computed pressure at the maximum and minimum model radii, respectively. $\frac{dp_N(r)}{dr}$ is the derivative of the normal pressure at radius r . This model has been computed for the bare 5nm gold nanoparticle at 900 K and 1000 K, and result in surface tension values of $751 \frac{mN}{m}$ and $617 \frac{mN}{m}$, respectively. These temperature bound the melting temperature and the surface tension results bound the published data of $742 \frac{mN}{m}$, again providing some validation of the MD model used.

4. Conclusions

This overview of simulation results for the alkanethiolate SAM coated gold nanoparticle has provided some insights into this system. For instance, from the diffusivity calculations, three distinct temperature ranges have been observed. These ranges could be different phases for the adsorbed SAMs, much like those observed on flat surfaces [23]. The radial density results have shown that the surface of the gold nanoparticle becomes corrugated as SAMs are adsorbed onto the surface, and a corrugation factor has been defined herein. These results have spurred closer inspection of the material system so that more properties and a phase diagram can be developed.

5. Acknowledgements

The authors would like to acknowledge the support received by the U.S. Army Major Shared Resource Center (MSRC) at the Aberdeen Proving Ground, MD. Additional support was provided by the National Institute for Standards Technology (NIST) and the University of Maryland at College Park.

References

- [1] M. P. Allen and D. J. Tildesley. *Computer Simulation of Liquids*. Oxford University Press Inc., New York, NY, 1987.

- [2] H. C. Andersen. RATTLE: A Velocity Version of the SHAKE Algorithm for Molecular Dynamics. *Journal of Computational Physics*, 52:24–34, 1983.
- [3] K. M. Beardmore, J. D. Kress, N. Gronbeck-Jensen, and A. R. Bishop. Determination of the headgroup-gold(111) potential surface for alkanethiol self-assembled monolayers by ab initio calculation. *Chemical Physics Letters*, 286:40–45, 1998.
- [4] M. S. Daw and M. I. Baskes. Embedded-atom method: Derivation and application to impurities, surfaces, and other defects in metals. *Physical Review B*, 29(12):6443–6453, 1984.
- [5] S. M. Foiles, M. I. Baskes, and M. S. Daw. Embedded-atom-method functions for the fcc metals Cu, Ag, Au, Ni, Pd, Pt, and their alloys. *Physical Review B*, 33(12):7983–7991, 1986.
- [6] H. Fukunaga, J. i. Takimoto, and M. Doi. A coarse-graining procedure for flexible polymer chains with bonded and nonbonded interactions. *Journal of Chemical Physics*, 116(18):8183–8190, 2002.
- [7] H. Grönbeck, A. Curioni, and W. Andreoni. Thiols and Disulfides on the Au(111) Surface: The Headgroup-Gold Interaction. *Journal of the American Chemical Society*, 122:3839–3842, 2000.
- [8] J. Hautman and M. L. Klein. Simulation of a monolayer of alkyl thiol chains. *Journal of Chemical Physics*, 91(8):4944–5001, 1989.
- [9] S. Jiang. Molecular simulation studies of self-assembled monolayers of alkanethiols on Au(111). *Molecular Physics*, 100(14):2261–2275, 2002.
- [10] W. L. Jorgensen, J. D. Madura, and C. J. Swenson. Optimized Intermolecular Potential Functions for Liquid Hydrocarbons. *Journal of the American Chemical Society*, 106:6638–6646, 1984.
- [11] C. L. Kelchner, D. M. Halstead, L. S. Perkins, N. M. Wallace, and A. E. DePristo. Construction and evaluation of embedding functions. *Surface Science*, 310:425–435, 1994.
- [12] U. Landman and W. D. Luedtke. Small is different: energetic, structural, thermal, and mechanical properties of passivated nanocluster assemblies. *Faraday Discussions*, 125:1–22, 2004.
- [13] B. Lee and K. Cho. Extended embedded-atom method for platinum nanoparticles. *Surface Science*, 600:1982–1990, 2006.
- [14] K. S. S. Liu, C. W. Yong, B. J. Garrison, and J. C. Vickerman. Molecular Dynamics Simulations of Particle Bombardment Induced Desorption Processes: Alkanethiolates on Au(111). *Journal of Physical Chemistry B*, 103:3195–3205, 1999.
- [15] W. D. Luedtke and U. Landman. Structure, Dynamics, and Thermodynamics of Passivated Gold Nanocrystallites and Their Assemblies. *The Journal of Physical Chemistry*, 100(32):13323–13329, 1996.
- [16] R. Mahaffy, R. Bhatia, and B. J. Garrison. Diffusion of a Butanethiolate Molecule on a Au(111) Surface. *Journal of Physical Chemistry B*, 101:771–773, 1997.
- [17] P. K. Maiti, Y. Lansac, M. A. Glaser, and N. A. Clark. Self-Assembly in Surfactant Oligomers: A Coarse-Grained Description through Molecular Dynamics Simulations. *Langmuir*, 18:1908–1918, 2002.
- [18] J. Mei, J. W. Davenport, and G. W. Fernando. Analytic embedded-atom potentials for fcc metals: Application to liquid and solid copper. *Physical Review B*, 43(6):4653–4658, 1991.
- [19] S. J. Plimpton. Fast Parallel Algorithms for Short-Range Molecular Dynamics. *Journal of Computational Physics*, 117:1–19, 1995.
- [20] T. J. Raeker and A. E. DePristo. Theory of chemical bonding based on the atom-homogeneous electron gas system. *International Reviews in Physical Chemistry*, 10(1):1–54, 1991.
- [21] B. Rai, P. Sathish, C. P. Malhotra, Pradip, and K. G. Ayappa. Molecular Dynamic Simulations of Self-Assembled Alkylthiolate Monolayers on an Au(111) Surface. *Langmuir*, 20:3138–3144, 2004.
- [22] J. Rowlinson and B. Widom. *Molecular Theory of Capillarity*. Oxford University Press, Oxford, England, 1982.
- [23] F. Schreiber. Self-assembled monolayers: from ‘simple’ model systems to biofunctionalized interfaces. *Condensed Matter*, 16:R881–R900, 1994.
- [24] A. V. Shevade, J. Zhou, M. T. Zin, and S. Jiang. Phase Behaviour of Mixed Self-Assembled Monolayers of Alkanethiols on Au(111): A Configurational-Bias Monte Carlo Simulation Study. *Langmuir*, 17:7566–7572, 2001.
- [25] M. S. Stave, D. E. Sanders, T. J. Raeker, and A. E. DePristo. Corrected effective medium method. V. Simplifications for molecular dynamics and Monte Carlo simulations. *Journal of Chemical Physics*, 93(6):4413–4426, 1990.
- [26] S. M. Thompson, K. E. Gubbins, J. P. R. B. Walton, R. A. R. Chantry, and J. S. Rowlinson. A molecular dynamics study of liquid drops. *Journal of Chemical Physics*, 81(1):530–542, 1984.
- [27] V. Tries, W. Paul, J. Baschnagel, and K. Binder. Modeling polyethylene with the bond fluctuation model. *Journal of Chemical Physics*, 106(2):738–748, 1997.
- [28] A. F. Voter and S. P. Chen. High temperature ordered intermetallic alloys. In *Characterization of Defects in Materials*, volume 82, page 175, Pittsburgh, 1987. Materials Research Society.
- [29] L. Zhang, W. A. Goddard III, and S. Jiang. Molecular simulation study of the c(4x2) superlattice structure of alkanethiol self-assembled monolayers on Au(111). *Computers in Chemical Engineering*, 22(10):1381–1385, 2002.